Electronic Supplementary Material (ESI) for Journal of Materials Chemistry B.

Supporting Information

Biodegradable MnFe-hydroxide Nanocapsules to enable Multi-therapeutics Delivery and Hypoxia-Modulated Tumor Treatment

Linhua Liao,[†a] Dong Cen,[†b] Yike Fu,[a] Bin Liu,[a] Chao Fang,[a] Yifan Wang,[b] Xiujun Cai,[b] Xiang Li,*[a] Hao Bin Wu,*[a] and Gaorong Han[a]

[a.] State Key Laboratory of Silicon Materials, School of Materials Science and Engineering, Zhejiang University, Hangzhou 310027, P.R. China

[b.] Key Laboratory of Endoscopic Technique Research of Zhejiang Province, Sir Run Shaw Hospital, Zhejiang University, Hangzhou 310016, P. R. China

† Authors with equal contribution

*Corresponding authors: xiang.li@zju.edu.cn (XL), hbwu@zju.edu.cn (HBW).

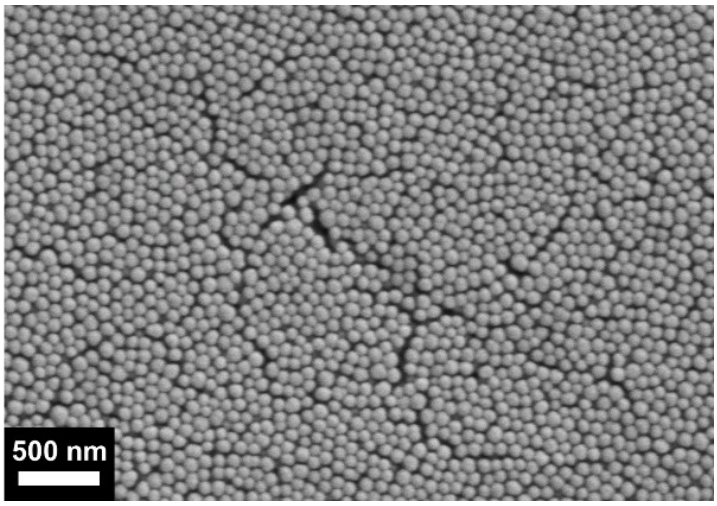

Figure S1. SEM image of solid SiO_2 nanoparticles as hard template.

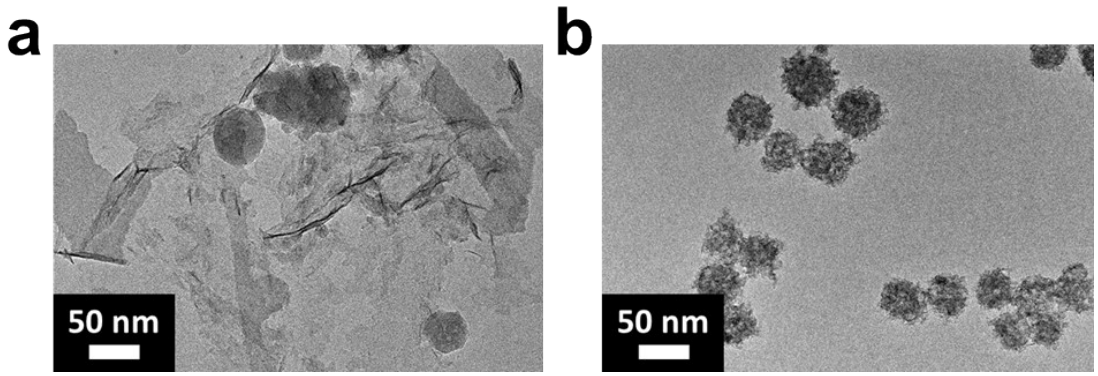

Figure S2. TEM images of the nanoparticles synthesized when only using (a) Mn^{2+} or (b) Fe^{3+} precursor.

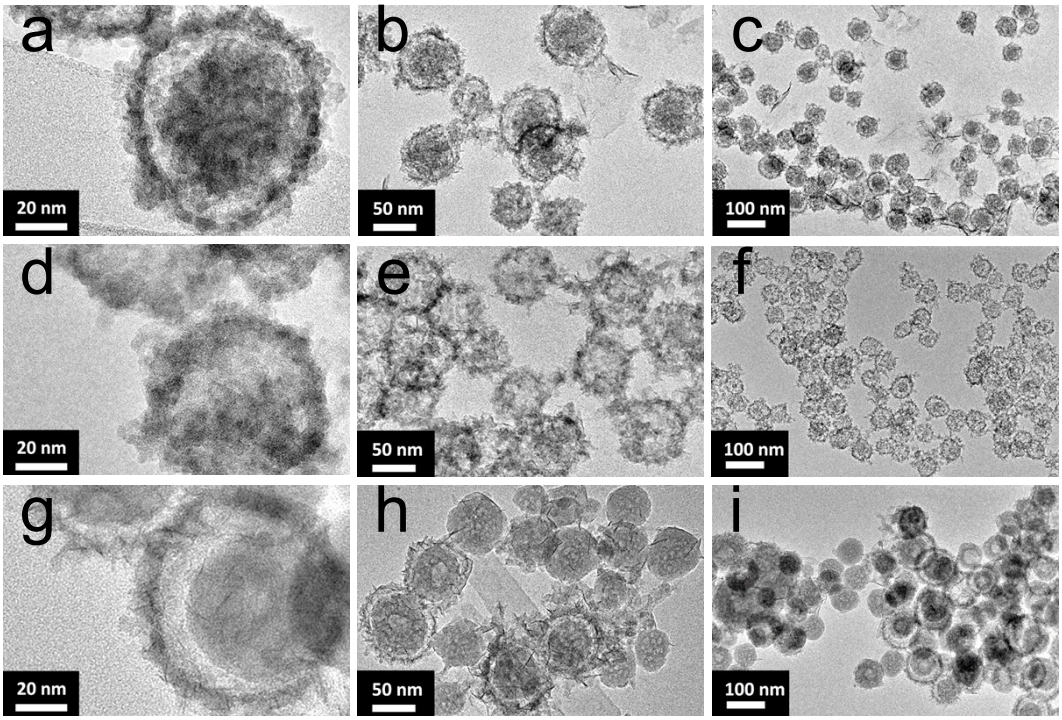

Figure S3. TEM images of SiO_2@MnFe(OH)$_x$ nanoparticles after incubating in $NH_3 \cdot H_2O$ solution with various concentrations: (a)~(c) 0.25 M, (d)~(f) 0.5 M, (g)~(i) 1.5 M at 120 ℃ for 24h.

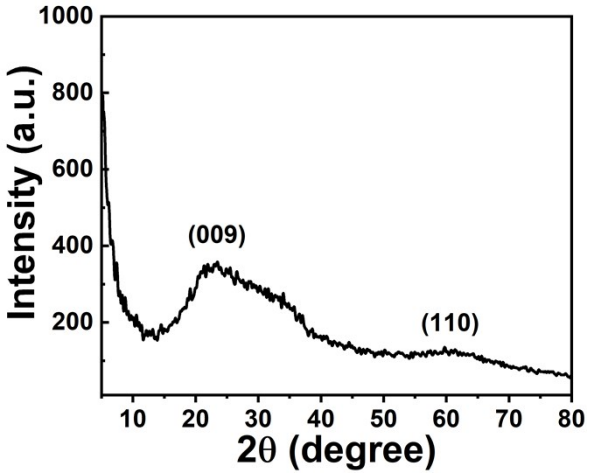

Figure S4. XRD pattern of H-MnFe(OH)$_x$ nanocapsules.

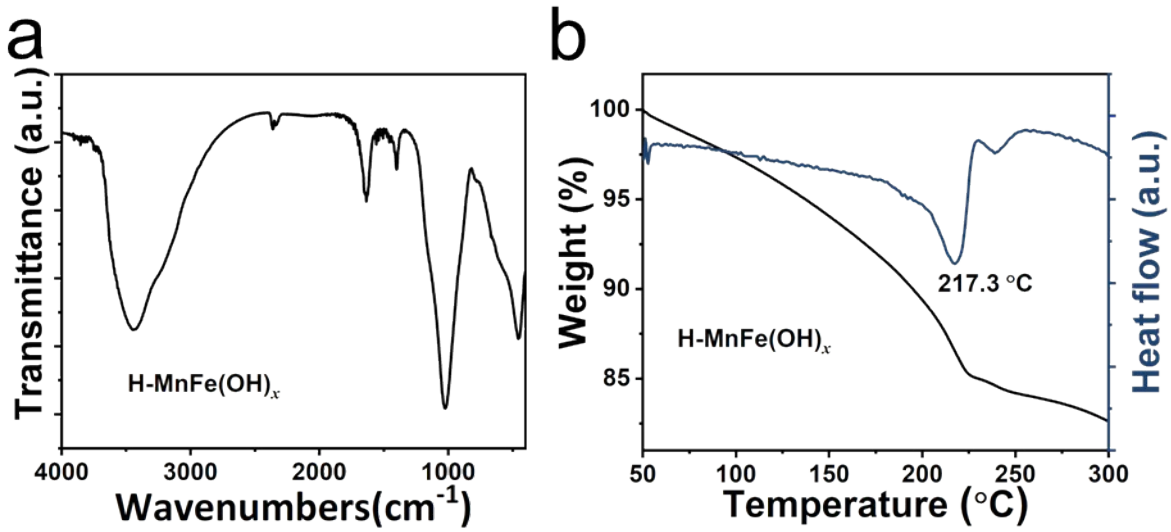

Figure S5. (a) FTIR spectrum and (b) TGA-DSC curve of H-MnFe(OH)$_x$ nanocapsules.

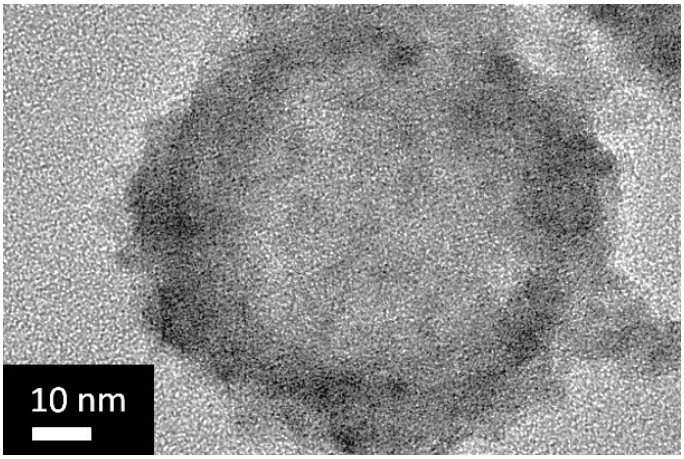

Figure S6. HRTEM image of H-MnFe(OH)$_x$ nanocapsules.

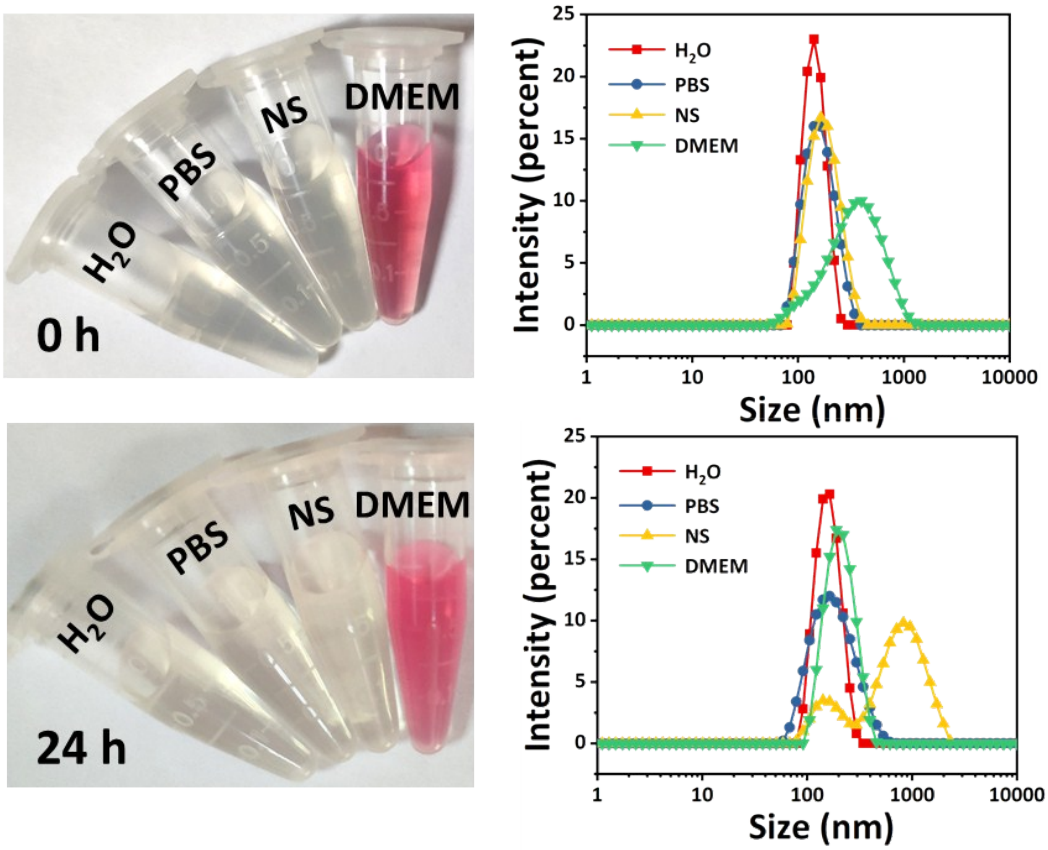

Figure S7. Digital photographs and corresponding size distribution of H-MnFe(OH)$_x$ in water, PBS, normal saline (NS) and cell culture medium (DMEM) at 0 and 24 h.

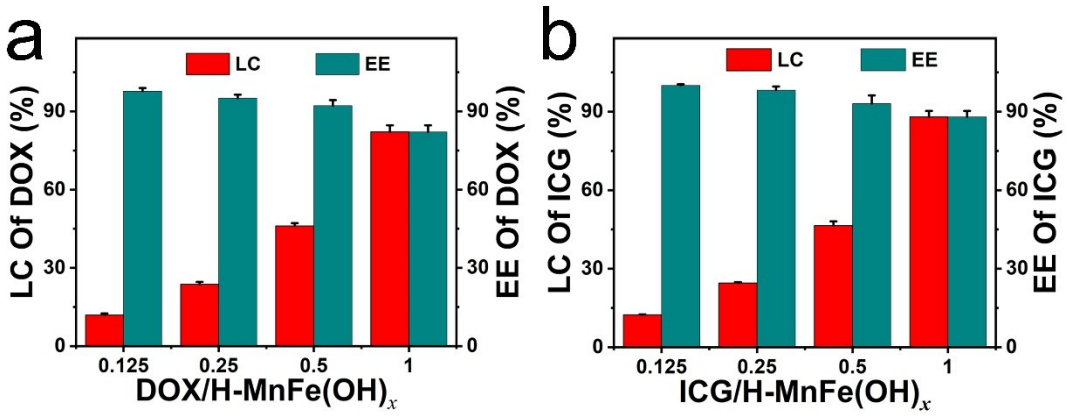

Figure S8. LC and EE of (b) DOX and (c) ICG into H-MnFe(OH)x with various mass ratios *via* individual loading.

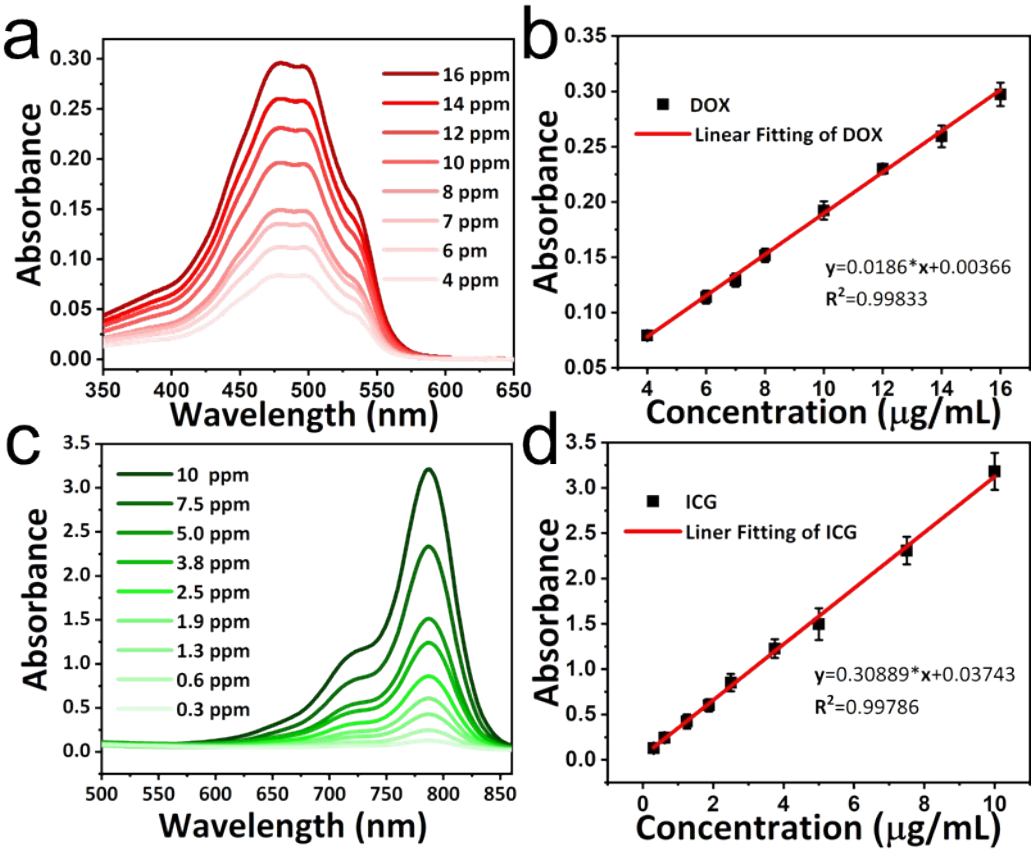

Figure S9. (a) UV−vis−NIR spectra and (b) the standard curve of DOX at different concentrations. (c) UV−vis−NIR spectra and (d) the standard curve of ICG solutions at different concentrations.

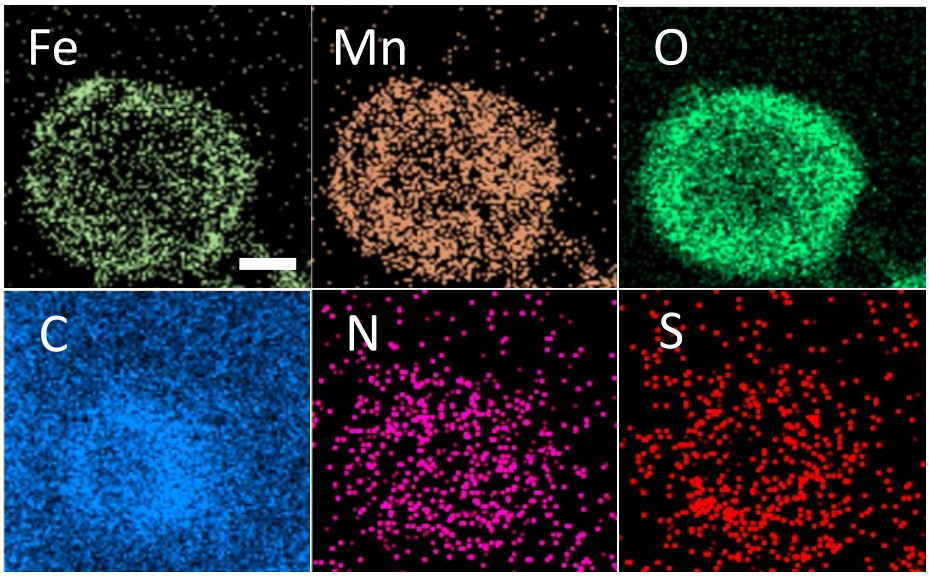

Figure S10. Elemental mapping for DOX&ICG/ H-MnFe(OH)$_x$. Scale bar (20 nm).

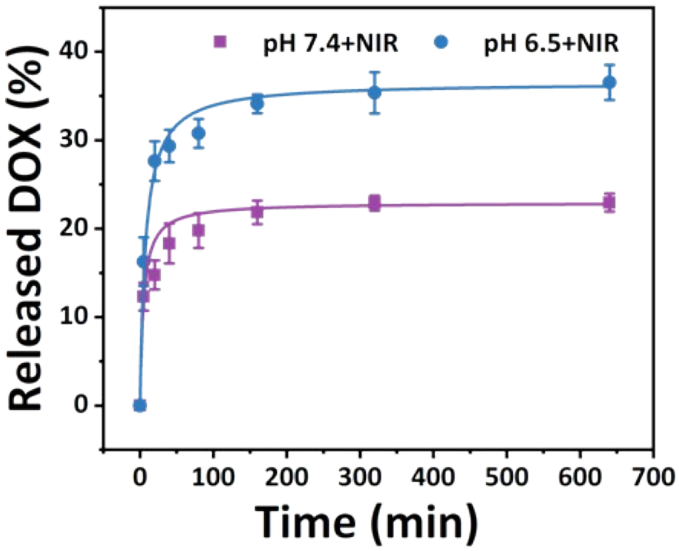

Figure S11. DOX release from DOX&ICG/ H-MnFe(OH)$_x$ in PBS at pH = 7.4, and pH = 6.5 with 808 nm irradiation (0.69 W cm^{-2}).

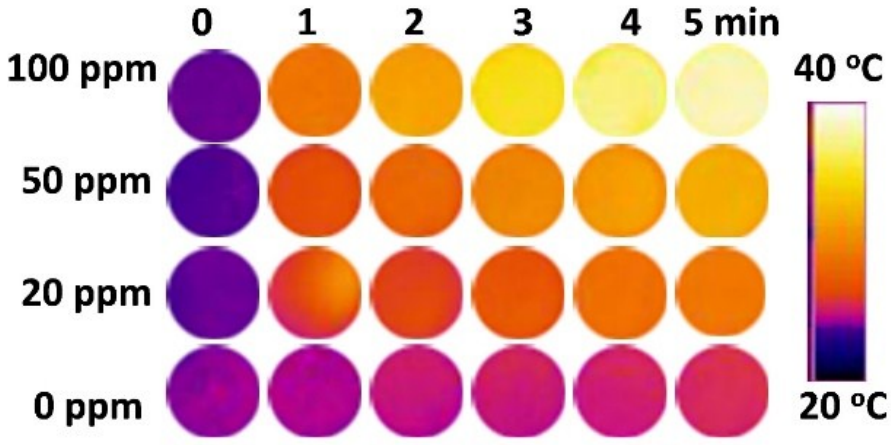

Figure S12. Temperature photographs of DOX&ICG/ H-MnFe(OH)$_x$ at various concentrations under NIR irradiation for 0-5 min (808 nm, 0.69 Wcm^{-2}).

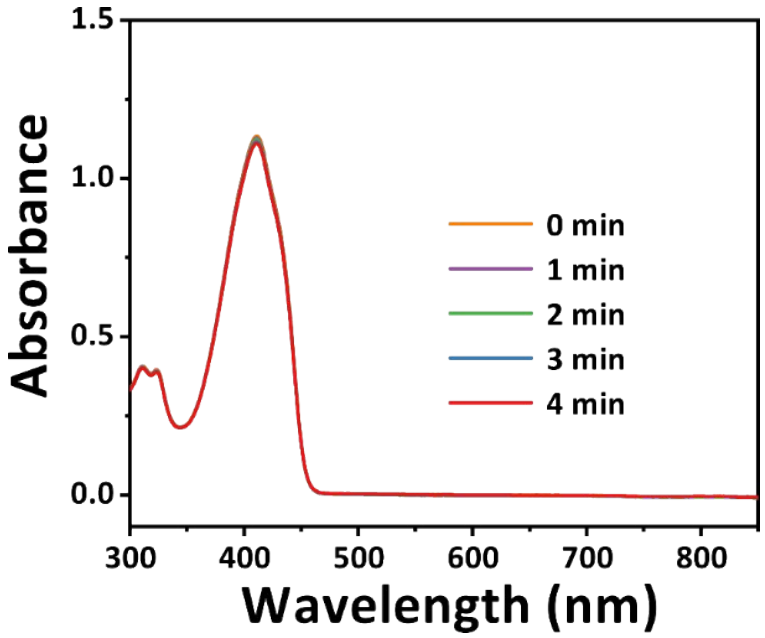

Figure S13. UV−vis−NIR absorption spectra of DPBF upon 808 nm laser irradiation (0.69 W cm^{-2}).

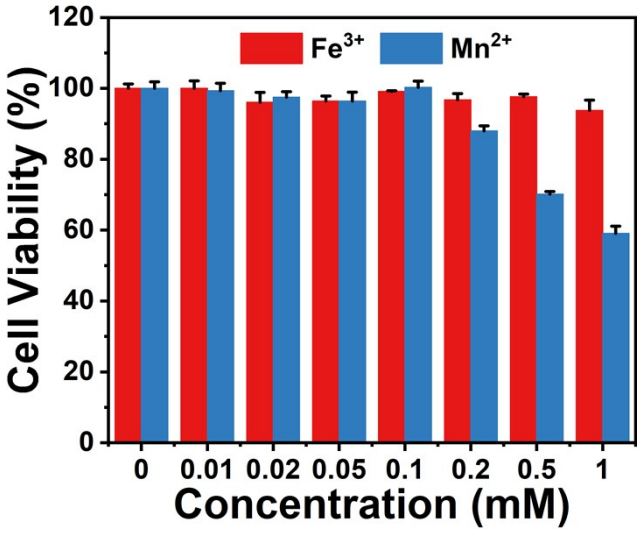

Figure S14. The viability of 4T1 cells incubated with various concentrations of Fe^{3+} or Mn^{2+}.

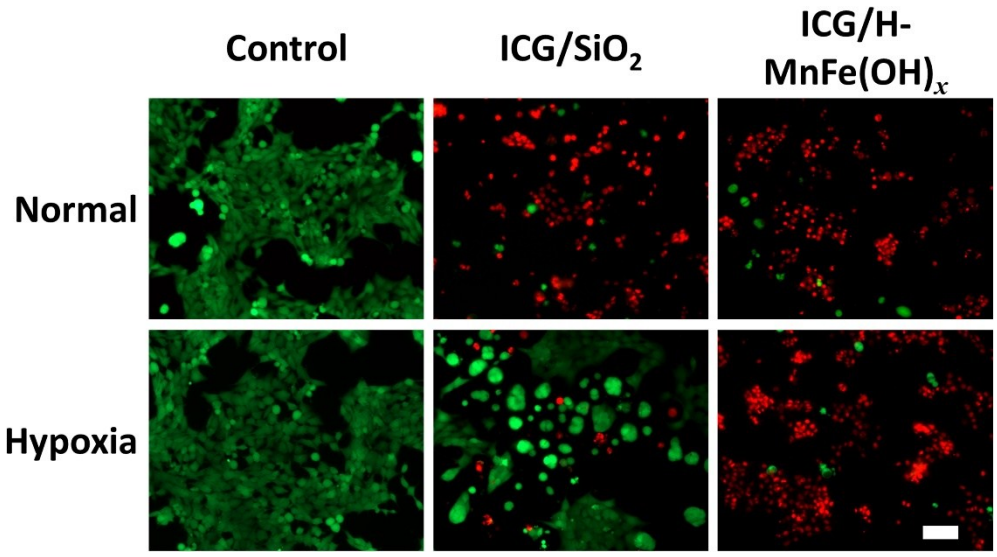

Figure S15. Fluorescence images of 4T1 cells stained with calcein-AM (green, live cells) and propidium iodide (red, dead cells) after treated with ICG/SiO_2 and ICG/LDH samples upon NIR irradiation in N_2 or O_2 atmospheres. Scale bar = 50 μm.

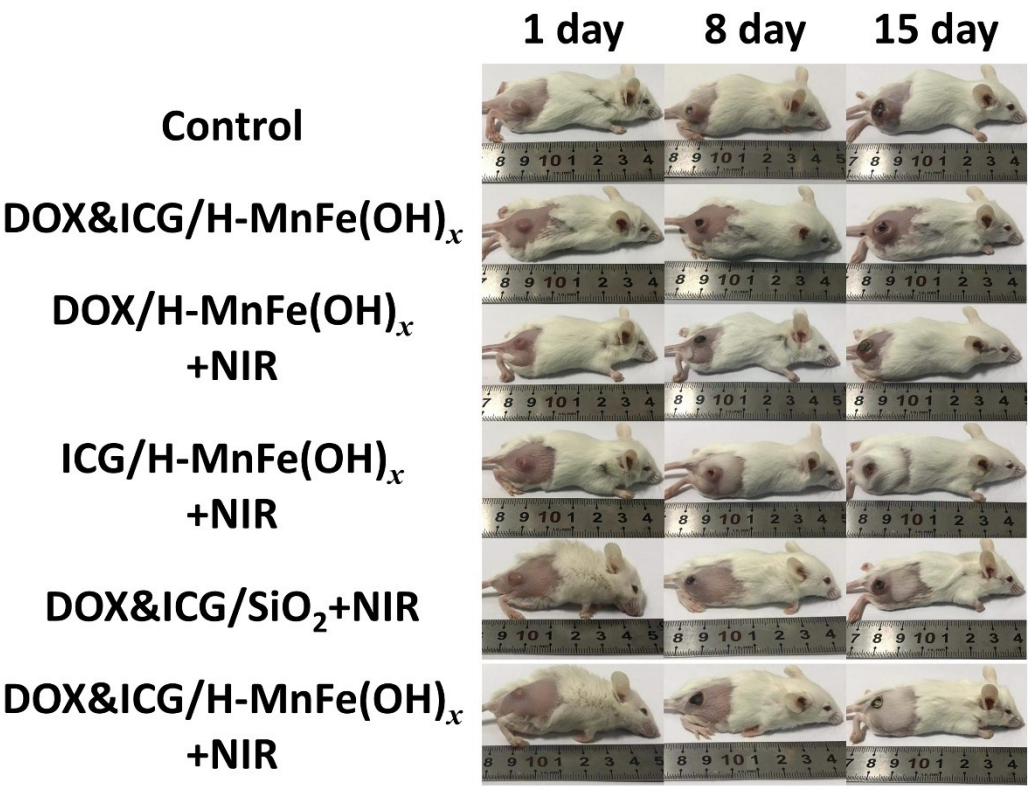

Figure S16. Digital photographs of the mice on day 1, 8 and 15 after various treatments.